

MRI-DWI improves the early diagnosis of brain abscess induced by *Candida albicans* in preterm infants

Jian Mao¹, Juan Li¹, Dan Chen¹, Jing Zhang¹, Ya-Nan Du¹, Ying-Jie Wang¹, Xin Li¹, Rui Wang¹, Li-Ying Chen², Xiao-Ming Wang²

¹Department of Pediatrics, Shengjing Hospital, China Medical University, Shenyang 110004, China; ²Department of Radiology, Shengjing Hospital, China Medical University, Shenyang 110004, China

Correspondence to: Jian Mao, MD. Department of Pediatrics, Shengjing Hospital, China Medical University, Shenyang 110004, China.
Email: maoj@sj-hospital.org.

Objective: To investigate the diagnostic value of magnetic resonance imaging (MRI) in brain abscess induced by invasive fungal infection (IFI) of the central nervous system.

Methods: The clinical data of eight preterm infants with IFI of the central nervous system were retrospectively analyzed. All these eight children received three sequential brain MRI modes T1WI, T2WI and DWI during hospitalization and after discharge.

Results: All these eight preterm infants were infected with *Candida albicans*, seven of which were manifested by brain abscess and four were accompanied by meningitis. MRI of seven infants with brain abscess indicated extensive invasion including involvement of subcortical white matter, deep periventricular white matter and semiovale center white matter. MRI examination was conducted within 11 d following infection on four cases and showed diffuse or multiple miliary nodules, hyper-intense signal on DWI, while insignificant signal changes on T1WI and T2WI. DWI signal nearly disappeared three weeks later. T1WI/T2WI signal changed most significantly 2-4 weeks following infection, with nodules ring-shaped, hyper-intense signal around T1WI and hypo-intense signal in the center. Signal on T2WI was just on the opposite. Severe cases presented fusion of different degrees. Significant enhanced effect was observed on T1WI. Four weeks later, the lesion gradually became fewer and smaller on T1WI, transferred into dot or line-like hyper-intense signal and presented obviously hypo-intense signal on T2WI. Dynamic MRI of two cases showed delayed myelination and corpus callosum thinning.

Conclusion: MRI-DWI and dynamic MRI changes can improve the early diagnosis of brain abscess induced by *Candida albicans* in preterm infants.

Keywords: Brain abscess; *Candida albicans*; magnetic resonance imaging; preterm infants

Submitted Jan 20, 2012. Accepted for publication Feb 27, 2012.

doi: 10.3978/j.issn.2224-4336.2012.02.04

View this article at: <http://www.thetp.org/article/view/1092/1399>

Introduction

Late-onset neonatal sepsis is becoming a leading factor dominating quality of life in very low-birth-weight (VLBW) and extremely-low-birth-weight (ELBW) infants, and invasive fungal infection (IFI) has become the third leading cause of late-onset sepsis (1). IFI accounts for 10% of all cases of nosocomial sepsis in very-low-birth weight (VLBW: <1,500 g) infants, which may be fatal in 25-50% of cases (2). However, Invasive *Candida* infection is an

increasingly important cause of morbidity and mortality in the neonatal intensive care unit (3). Neonatal candidemia occurs in 4-15% of extremely low birth weight infants (4,5). Meningitis occurs in 5-9% of patients with candidemia, a few infants with *Candida* meningitis (4%) present ventriculitis or brain abscess (3,4). Although blood-borne infection is an important pathway to induce invasive fungal infection of the central nervous system (CNS-IFI), the sensitivity of microbial examination for cerebrospinal fluid (CSF) remains low (6-8) and few studies have objectively

evaluated the normal values of biochemical and cytological examination results of CSF and their clinical significances in newborns with different degrees of maturity (9). Thus, early diagnosis of CNS infection is very difficult. Previous studies on diagnosis of neonatal CNS-IFI involve to the ultrasound changes of the ventricular system rather than the parenchymal brain (10-13). Recently, interest focus on brain magnetic resonance imaging (MRI) to detect multiple brain parenchyma micro abscesses (3). Changes in imaging characteristics may provide objective criteria for diagnosis and prognosis of neonatal CNS-IFI.

Diffusion-weighted MRI (DWI) is a functional MR imaging technique that uses differences in the extracellular movement of water protons to discriminate between tissues of varying cellularity. The application of MRI in the diagnosis of cerebral abscesses has been reported (3). In many reports, scanning sequences were only limited to routine T1WI/T2WI (13-16), and there is few observation on the diffusion-weighted imaging (MRI-DWI) and its dynamic changes.

In this study, the value of brain MRI was investigated combining CSF and its clinical manifestations through description of the manifestations and features of brain MRI with different sequences in eight preterm infants admitted to our hospital due to CNS-IFI.

Materials and methods

Patients

Eight preterm infants admitted to our hospital due to CNS-IFI in the past two years were included in this study. These patients included six males and two females with the gestational age of 31.5 ± 1.8 (range, 29-34) weeks and birth weight of 1416 ± 514 (range, 900-2,400) g. These eight preterm infants consisted of six VLBW infants and two ELBW infants; the major primary diseases were respiratory distress syndrome (RDS, $n=7$) and intestinal malrotation ($n=1$). All seven patients with RDS underwent surfactant (Curosurf) treatment; five of them received invasive mechanical ventilation and six received nasal continuous positive airway pressure (nCPAP). All patients received intravenous nutrition using a peripherally inserted central catheter (PICC) for an average of 25 ± 11 (range, 12-48) d. Third-generation cephalosporin and carbapenem antibiotics were commonly used for infection treatment and the onset time of IFI (based on the time obtaining a positive result in fungal cultivation) was 17.4 ± 8.1 (range, 11-36) d (Table 1).

Diagnostic criteria

Diagnostic criteria of IFI include: (I) clinical manifestations: low response, feeding difficulties, grey complexion, apnea, and sustained reduction in platelet count; (II) fungal growth during sterile body fluid cultivation; and (III) responds to anti-fungal treatment but not to antibiotic treatment (17).

Diagnostic criteria of CNS-IFI (18): established IFI diagnosis, positive for CSF cultivation or increased CSF white blood cell (WBC) count and positive for cultivation of other body fluid; or normal for CSF cultivation but positive for cultivation of other sterile body fluid, excluding MRI changes induced by other causes and responds to anti-fungal treatment.

Bacterial cultivation and detection of plasma 1,3- β -D-glucan

Routine blood, urine, and CSF tests, bacteriological cultivation, and mycological cultivation were performed for all IFI patients when they developed clinical manifestations of sepsis accompanied with increased CRP and declined platelet count. When IFI was confirmed, dynamic monitoring of CRP, counting of WBC and platelets in peripheral blood, and measurement of plasma 1,3- β -D-glucan levels were performed. Fungal cultivation was performed using BD-9240 Automated Blood Fungal Culture Instrument with fluorescence detection. Plasma 1,3- β -D-glucan analysis was carried out using the MB-80 microbiological dynamic monitoring system. The GKT-5Mset dynamic detection kit was provided by the Beijing Gold Mountainriver Tech Development Co., Ltd. The level of 1,3- β -D-glucan >20 pg/L was regarded as clinically significant.

Brain MRI

All pediatric patients underwent brain MRI, among whom one patient received contrast-enhanced MRI scan. Apart from one patient scanned with the 1.5 T GE superconducting MRI diagnostic instrument, other patients were all scanned with the 3.0 T Philips Intera Achieva superconducting MR instrument. Scanning sequences and parameters were as follows: T1WI: FFE CLEAR sequence TR/TE 126 ms/2.3 ms, Flip 80; T2WI: TSE SENSE sequence TR/TE 1856-3238 ms/80-100 ms, TSE Factor 15; diffusion-weighted imaging (DWI): DW SSh SENSE sequence TR/TE 2463 ms/48 ms, EPI Factor 45, b value

Table 1 Clinical data and laboratory test results of 8 pediatric patients with CNS-IFI

	Case 1	Case 2	Case 3	Case 4	Case 5	Case 6	Case 7	Case 8
Gestational age (weeks)	33 ⁺¹	32	33 ⁺³	34	31	29 ⁺⁴	29 ⁺⁶	29
Birth weight (g)	1,385	1,020	1,935	2,400	1,350	990	1,350	900
Gender	Female	Female	Male	Male	Male	Male	Male	Male
Delivery mode	Vaginal delivery	Cesarean section	Vaginal delivery	Cesarean section	Cesarean section	Cesarean section	Cesarean section	Cesarean section
Apgar score (1 min/5 min)	10/10	10/10	6/7	10/10	10/10	7/9	8/9	5/7
Usage of antibiotics	Ceftazidime/ imipenem	Mezlocillin/ imipenem	Ceftazidime/ cefepime/ vancomycin	Ceftazidime/ cefepime/ metronidazole	Mezlocillin/ imipenem	Mezlocillin/ ceftazidime	Ceftazidime/ meropenem	Mezlocillin/ meropenem
PICC intubation (d)	23	16	12	25	18	28	30	48
Mechanical ventilation (d)	5	14	-	-	6	6	7	-
NCPAP (d)	-	-	5	18	5	20	12	7
Time to IFI (d)	18	11	11	18	15	18	12	36
Peripheral blood								
WBC ($\times 10^9$ /L)	44.8	10.8	25.2	20.0	12.8	9.2	46.4	7.2
PLT ($\times 10^9$ /L)	171	8	45	55	18	59	46.0	16
CRP (mg/L)	8.3	138.0	78.0	16.0	26.5	62.0	21.5	68.5
1,3- β -D (pg/mL)	176.6	331.0	-	-	<5.0	3133.0	220.0	655.2
Treatment duration								
Fluconazole	3 weeks	2d	4 weeks	4 weeks	2 weeks	2 weeks	3 weeks	2 weeks
Amphotericin B	-	-	-	-	-	-	2 weeks	3 weeks
Other involvement	Skin abscesses/ arthritis	Pneumonia	Retinal hemorrhage	Endophthalmitis/ arthritis	Pneumonia	Renal abscess/ pneumonia	Pneumonia/ skin abscesses	Pneumonia
Primary disease	RDS	RDS	RDS/ICH	Malrotation of intestine	RDS	RDS	RDS	RDS,BPD
Outcome of hospitalization	Discharged	Giving up treatment	Discharged	Discharged	Discharged	Discharged/ readmission due to renal failure	Discharged	Hospitalized due to BPD

Notes: RDS, respiratory distress syndrome; ICH, intracerebral hemorrhage; BPD, bronchopulmonary dysplasia.

1,000, gradient magnetic field applied in three directions; Scan matrix 256 \times 182/256, field of view 17 cm \times 17 cm - 23 cm \times 23 cm, and slice thickness 4-5 mm. Phenobarbital sodium 10 mg/kg was slowly injected intravenously prior to scanning for sedation and the transcutaneous oxygen saturation was monitored during the examination. All MRI results were interpreted by two radiologists who were blind to the clinical history of these patients.

Treatment

All pediatric patients received a variety of antibiotic therapies and PICC before the diagnosis of IFI. After IFI was confirmed, they were firstly treated by fluconazole at an initial dose of 12 mg/kg, followed by intravenous injection of 6 mg/kg daily. Two cases were also given amphotericin B liposome at a daily dose of 5 mg/kg. The liver function,

Table 2 Microbiology, CFS, and clinical diagnosis of 8 pediatric patients with CNS-IF

Case	CSF			Fungal cultivation					Clinical diagnosis
	WBC ($\times 10^6/L$)	Glu (nmol/L)	Protein (g/L)	Chlorides (nmol/L)	CSF	Blood	Urine	PICC tube	
1	2	1.21	1.2	129	-	+	-	-	Multiple brain abscesses
2	10	0.99	2.9	121	-	+	-	-	Multiple brain abscesses
3	82	1.60	2.1	120	-	+	-	+	Multiple brain abscesses/ meningitis
4	90	1.54	1.4	120	-	+	-	-	Multiple brain abscesses/ meningitis
5	5	2.41	1.5	117	-	+	-	-	Multiple brain abscesses
6	150	1.84	3.0	100	-	+	+	+	Multiple brain abscesses/ meningitis
7	2	2.14	2.2	107	-	+	+	-	Multiple brain abscesses
8	52	1.07	1.4	105	-	+	-	+	Meningitis

WBC and platelet count in peripheral blood and changes in plasma electrolyte levels were stringently monitored during the treatment.

Results

Clinical manifestations and laboratory test results

Seven of these eight CNS-IFI patients were manifested by brain abscess, among whom three were also manifested by meningitis and one by meningitis alone. *Candida albicans* was detected by blood fungal cultivation and was negative by CSF cultivation. Among three patients who had undergone PICC, urine cultivation showed *Candida albicans* in two cases. In four patients: CSF WBC $>45 \times 10^6/L$, CSF glucose 1.6 ± 0.5 (range, 0.99-2.41) mmol/L, protein 1.96 ± 0.70 (range, 1.2-3.0) g/L, chloride 114.8 ± 9.8 (range, 100-129) mmol/L (Table 2). After the fungal infection, three cases had blood WBC $>25 \times 10^9/L$ and the remaining parameters were normal; seven had significantly increased CRP and six had platelet count $<100 \times 10^9/L$; among six patients who had undergone plasma 1-3- β -D-glucan analysis, five had significantly increased plasma 1-3- β -D-glucan. Apart from nervous system involvement, lung (n=4), skin (n=2), joint (n=2), eyes (n=2) and kidney (n=1) were also affected in some patients. One patient gave up

treatment, and the remaining seven patients were clinically cured and discharged. One case with the longest follow-up period is 18-month-old now and grows normally; the other seven patients has been followed up for six months and show delayed motor development.

MRI manifestations

MRI of the seven pediatric patients with brain abscess showed a wide range of invasions, and the affected regions were as follows: subcortical white matter, deep periventricular and semiovale center white matter (n=7), corpus callosum (n=1), deep gray matter of the basal ganglia (n=3), cerebellum (n=2), and brainstem (n=1). In four cases whose MRI was conducted within 11 d (mean: 8.3 d) following infection, diffuse or multiple miliary nodules showed high-signal changes on DWI, and the earlier MRI was conducted the more obvious DWI signal was. However, T1WI/T2WI signal changed most significantly 2-4 weeks following infection, with nodules ring-shaped in four cases, showing high signal intensity in the rim of the lesion with low signal intensity in the center. Signals on T2WI were just the opposite, and showed certain degree of fusion in severer cases. Significant enhanced effect was observed on T1WI. DWI signals nearly disappeared three

Table 3 Dynamic MRI changes in 8 pediatric patients with CNS-IFI changes

Case	Duration of infection (d)	Time of first MRI (d)	Injured site	Change of the first MRI signal	Dynamic MRI changes
1	18	28	Subcortical white matter, periventricular white matter, and semi-oval center white matter, and basal ganglia	Diffuse miliary nodules, hyper-intense signal on DWI and T1WI and relatively low signal on T2WI; the signal was most significant on T1WI, with low signal at center	On day 31, some lesions fused, with ring-shaped enhancement; on Day 40, the changes disappeared on DWI, nearly disappeared on T2WI, and were still obvious on T1WI; and on Day 90, T1WI showed a few hyperintense signals, while no abnormality was observed on DWI and T2WI, and delayed myelination was also observed
2	11	15	Cortical and subcortical white matter, periventricular white matter, and semi-oval center white matter, and basal ganglia	Diffuse miliary nodules with varied sizes, which were most obvious on DWI; Edema-like changes were observed on T1WI/T2WI. For larger lesions, T1WI showed hyperintense signals at the rim and hypointense signals in the center, whereas T2WI showed the opposite signals	The patient did not receive a second MRI because she gave up treatment
3	11	36	Subcortical region, periventricular white matter, and basal ganglia	DWI and T2WI showed no abnormal signal. Multiple miliary hyperintense signals was detected on T1WI	The patient was under follow-up but has not received a second MRI
4	18	44	Periventricular white matter	DWI and T2WI showed no abnormal signal. Multiple miliary hyperintense signals was detected on T1WI	The patient was under follow-up but has not received a second MRI
5	15	38	Subcortical white matter, semi-oval center white matter, and cerebellum	MRI showed multiple miliary ring-shaped hyper-intense signals on T1WI, hypo-intense signal on T2WI, and hyper-intense signal on some DWI	On day 53, the abnormal signal on DWI disappeared, and the miliary lesions on T1WI/T2WI became smaller. The patient is under follow-up
6	18	26	Subcortical white matter, periventricular white matter, and semi-oval center white matter, and brain stem	MRI showed diffuse dot-like abnormal signals, which were hyper-intense on DWI, obviously low on T2WI and not obvious on T1WI	On day 40, the abnormal signals became fewer on DWI but increased on T1WI; they were still hypo-intense on T2WI. On Day 61, no abnormal signal was detected on DWI, and abnormal signals on T1WI/T2WI became smaller and fewer
7	12	23	Subcortical white matter, periventricular white matter, and semi-oval center white matter Corpus callosum, basal ganglia, and cerebellum	MRI showed diffuse miliary nodules, with hyper-intense signal on DWI/T1WI and hypo-intense signal on T2WI. Some nodules fused or were ring-shaped	On day 64, the abnormal signal disappeared on DWI, decreased on T1WI (dotted line-shaped high signal), and became obviously hypo-intense on T2WI. No myelination of the internal capsule was observed. On Day 100, scattered dot-shaped hypo-intense signals were detected on DWI, whereas the signals of the lesions on T1WI and T2WI remained unchanged. The internal capsule became myelinated, and the corpus callosum became thinner. On Day 132, the MRI sequences changed as on Day 100. The patient had obviously delayed myelination
8	36	54	No parenchymal brain involvement was observed. The anterior horn of lateral ventricles slightly became bigger	No abnormal signal was detected on DWI, T1WI, or T2WI. No hydrocephalus was found	The patient was under follow-up but has not received a second MRI

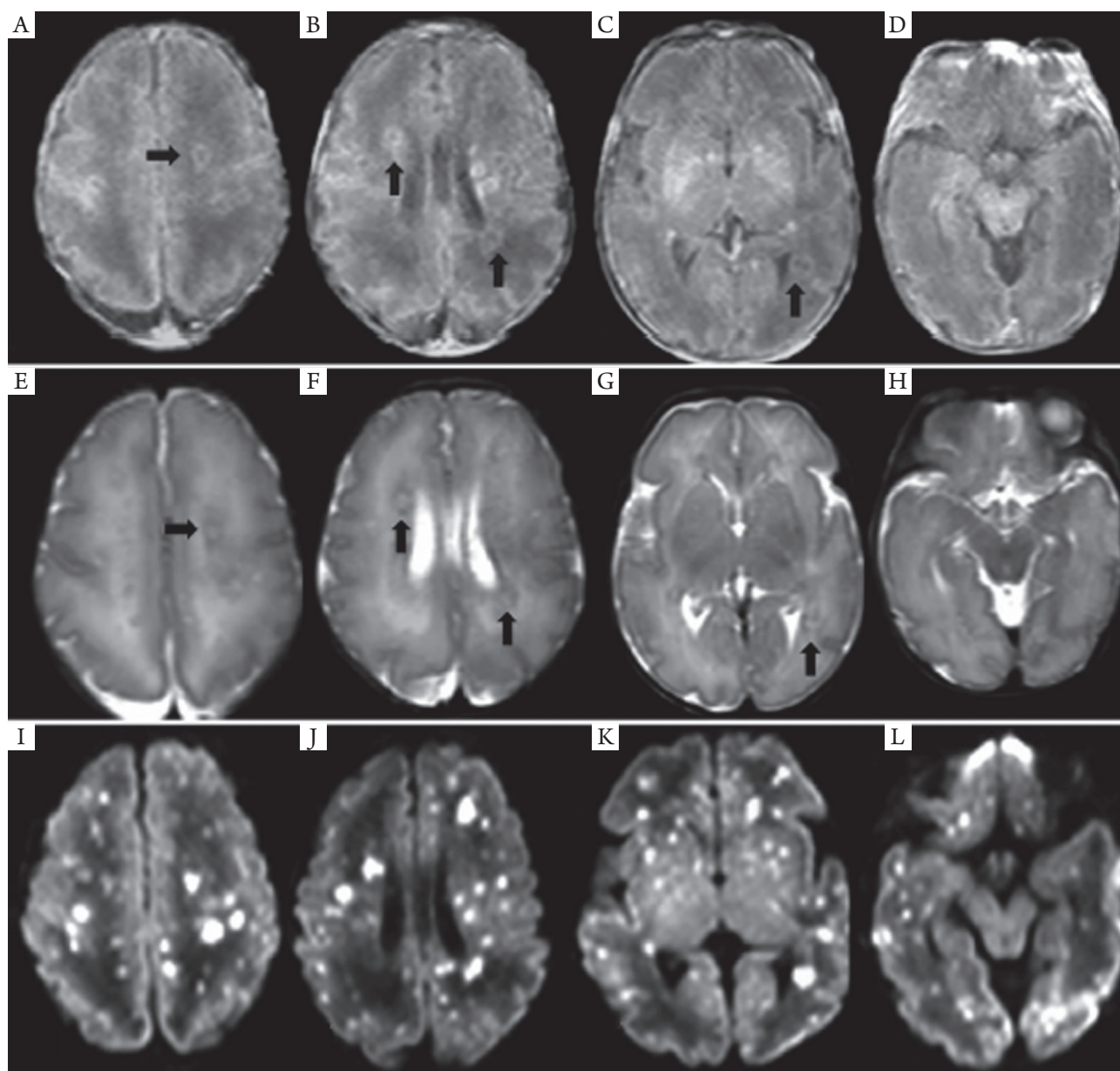


Figure 1 MRI findings of case 2 on day 15. On T1WI (A-D), the nodular lesions at semi-oval center white matter, periventricular white matter, and basal ganglia showed high signals, with nodules ring-shaped, hyper-intense signal at the rim, and hypo-intense signal in the center (arrow). On T2WI (E-H), the signal changes were on the opposite to T1WI. On DWI (I-L), wider involvement and more obvious signal changes, with diffuse nodular hyper-intense signal.

weeks later. Four weeks later, the lesion gradually became fewer and smaller on T1WI, transferred into dot or line-like hyper-intense signal, and presented obviously hypo-intense signal on T2WI. Dynamic MRI of two cases showed delayed myelination and corpus callosum thinning. (Table 3, Figures 1,2).

Discussion

Early diagnosis and rational treatment of CNS-IFI in preterm infants remains a challenge for physicians. The clinical manifestations of CNS-IFI are difficult to be distinguished from bacterial sepsis or meningitis. In addition,

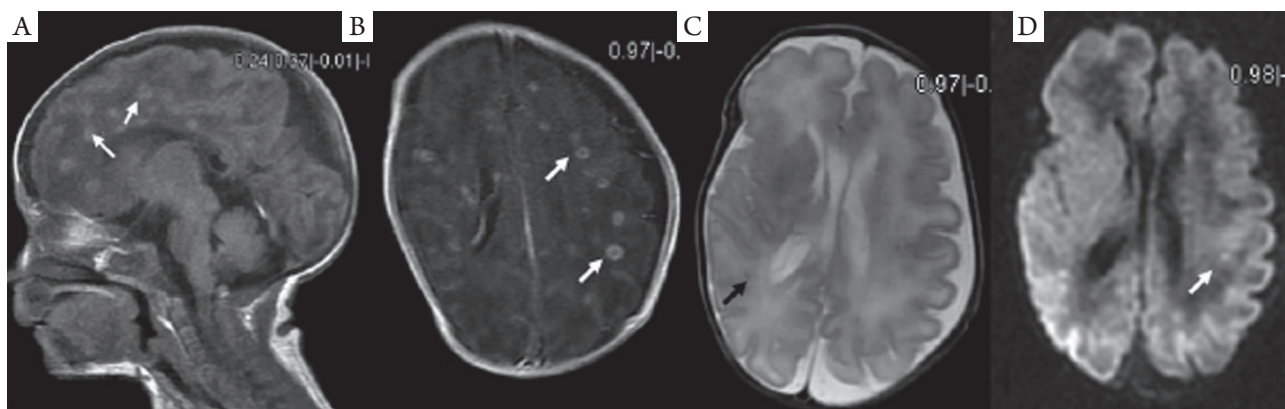


Figure 2 MRI findings of case 2 two weeks after infection. A. Multiple nodular hyperintense signals were found on the sagittate section of T1WI (arrow); B. The lesion showed obvious enhancement on T1WI (arrow); C-D. The changes of lesion signals were not as obvious as on T1WI.

the detection rate of pathogenic microorganisms is extremely low after infection, so it is difficult to be treated in a timely and appropriate manner. In our current study, all the eight pediatric patients with CNS-IFI had baseline candidemia and were negative for CSF cultivation, with CSF WBC $\geq 45 \times 10^6/L$ in four cases, glucose ≤ 1.3 mmol/L in three cases, and protein ≥ 1.7 g/L in four cases. Only four patients could be diagnosed as meningitis when the abnormal CSF was used as the diagnostic criteria; however, seven patients developed brain abscess, among whom one patient gave up treatment and the remaining six patients stopped antibiotic treatment and initiated anti-fungal treatment until they were discharged. Dynamic MRI changes in four cases supported the diagnosis of CNS-IFI. During the diagnosis of IFI-induced brain abscess, hyper-intense signal on early DWI and continuous hyper-intense signal on T1WI were important MRI findings. Extensive multi-site involvement supported the argument that blood-borne infection might be the main mechanism for the development of CNS-IFI.

Early diagnosis of CNS-IFI used to be difficult because it was highly dependent on the results of CSF cultivation for fungi and the results of routine biochemical examinations (19). This can be explained by the following reasons: (I) the fungus grows slowly. When the its level is < 1.0 mL in CSF specimen, the positive rate can be very low; (II) currently no well recognized normal value of CSF is available for preterm infants, and the diagnostic efficiency is low. For instance, for the diagnostic criteria of CSF WBC $> 25 \times 10^6/L$, glucose ≤ 0.56 mmol/L, and protein ≥ 2.5 g/L, it has a sensitivity of only 18%, although its specificity reaches 99.5% (9). Among CSF cultivation-confirmed pediatric patients with *Candida*

meningitis, 25% showed normal results during routine CSF tests and biochemical examinations (18,20); (III) the understanding of the pathological types of fungal infection of the central nervous system remains insufficient. Small abscess is one of the most important pathological types of fungal infection in adults and older children, whereas meningitis is less frequent (21,22). Although the incidence of meningitis may be higher in neonates than in older children, parenchymal brain involvement (brain abscess, and cerebral infarction), ventriculitis, and intraventricular fungal mass are not uncommon (10-16). Normal CSF is not sufficient to rule out the occurrence of brain abscess (23). Our current study has also shown that CNS-IFI could not be ruled out in patients with normal CSF, parenchymal brain involvement was an important pathological type of CNS-IFI, and imaging examination played an important role in its diagnosis.

Imaging and histological studies conducted by Huang *et al.* (13) on VLBW infants with CNS-IFI have found that there was involvement of either the brain parenchyma or ventricular system to varying degrees and multiple brain parenchymal echogenic ring enhancement and dense-echo mass of periventricular white matter fusion were the most common manifestations, which were pathologically confirmed as multiple small abscess and fused large abscess, respectively. MRI of one case showed diffuse miliary nodules widely distributed in the subcortical region, periventricular white matter, basal ganglia, and cerebellum, manifested by hyper-intense signal on T1WI.

MRI of seven pediatric patients in this study showed multiple miliary nodules, and four showed ring-shaped hyper-intense signal on T1WI, which were consistent

with Huang *et al.*'s findings (13). Contrast-enhanced MRI showed obvious ring-shaped enhancement, which was also in line with the pathological change into brain abscess. Pathologic examinations confirmed that the center of small abscess was hyphae and necrotic inflammatory cells, surrounded by proliferating endothelial cells and reactive glial cells as well as astrocytes with edema-like changes; larger abscess was surrounded by capillary proliferation and leukocyte infiltration (granulation tissue) (13). Therefore, abscess at its early stage or small abscess is manifested by hyper-intense signal nodules on T1WI, whereas larger abscess or abscess with central liquefaction/necrosis is manifested by ring-shaped nodules and enhancement effects. In other words, abscesses at different pathological stages have different imaging features. Study has shown that *Candida albicans* can pass through the blood-brain barrier without damaging the integrity of endothelial cells (24); meanwhile, the blood-brain barrier is insufficient. As a result, the neonates are prone to have multiple abscesses.

Of course, other pathogens, such as *Staphylococcus aureus*, *Citrobacter*, *Enterobacter cloacae*, *Escherichia coli*, and *Mycobacterium tuberculosis*, can also lead to brain abscess. However, in our series, the clinical manifestations, laboratory examinations, and clinical outcomes did not support the existence of these pathogens. No similar imaging features of other pathogens were identified (25,26). Dynamic MRI changes and the therapeutic efficacies of anti-fungal treatment for these pediatric patients fully supported the diagnosis of CNS-IFI. Thus, the existence of multiple small abscesses is also an important feature of neonatal CNS-IFI.

Dynamic MRI study found that early application of the DWI sequence might be helpful for the early detection of CNS-IFI-induced brain abscess. MRI-DWI study on adult brain abscess has indicated that hyper-intense signal of abscess on DWI after infection is more frequently seen after fungal infection. DWI signals at different stages might vary, namely, producing different apparent diffusion coefficient (ADC) values (27). Hyper-intense signal on DWI suggests that the restriction of water molecule movement in the lesion is due to endothelial cell swelling, increased proteins and lipids, and formation of abscess wall; hyper-intense signal on T1WI and hypo-intense signal on T2WI are related to cell damage and increased proteins and lipids within the abscess. An obvious enhancement effect under contrast-enhanced MRI is suggestive of the existence of abscess-like lesions. The lesion may become smaller on T1WI/T2WI during the restoration phase, but is still manifested as hyper-intense signal on T1WI and hypo-

intense signal on T2WI, which may be related with the glial cell proliferation. Dynamic MRI changes in the study are closely related to clinical outcomes. The extensive white matter involvement may be the major reason of delayed neurodevelopment. Also dynamic MRI can provide direct and objective evidence for the prognosis (or, the prediction of post-injury brain development). To our knowledge, no dynamic MRI study on CNS-IFI has been published. Early DWI multifocal hyper-intense signal combined with the manifestations of systemic fungal infection may provide clues for the early diagnosis of CNS-IFI.

Since prophylactic antifungal therapy is not clinically applied and 1,3- β -D-glucan is not applied for early infection monitoring, patients suspected to be with late-onset sepsis usually receive empirical antibiotic treatment first and thus often miss the chance of early diagnosis. Therefore, the "early" MRI changes mentioned in this study actually refers to the "acute phase" changes. Furthermore, all IFI cases in this study is caused by *Candida albicans* infection, so the result is not applicable to all fungal infections. Though, unfortunately, CSF cultivation showed negative results in all cases with CNS-IFI in this study, antibiotics were terminated before the initiation of anti-fungal treatment; therefore, the diagnosis can be regarded as "reliable" when combined with the clinical outcomes. Of course, it also emphasizes the necessity of MRI examination.

In conclusion, for suspected pediatric patients, this study shows that MRI should be performed not only for those with abnormal CSF cultivation results but also for those with normal results. MRI-DWI and dynamic MRI examination can play an important role in the diagnosis of cerebral abscess infection-induced by *Candida albicans* of premature infants.

Acknowledgements

None.

Footnote

Conflicts of Interest: The authors have no conflicts of interest to declare.

References

1. Stoll BJ, Hansen N. Infections in VLBW infants: studies from the NICHD Neonatal Research Network. *Semin Perinatol* 2003;27:293-301.
2. Tezer H, Canpolat FE, Dilmen U. Invasive fungal infections

- during the neonatal period: diagnosis, treatment and prophylaxis. *Expert Opin Pharmacother.* 2012;13:193-205.
3. Ancalle IM, Rivera JA, García I, et al. *Candida albicans* meningitis and brain abscesses in a neonate: a case report. *Bol Asoc Med P R* 2010;102:45-8.
 4. Benjamin DK Jr, Poole C, Steinbach WJ, et al. Neonatal candidemia and end-organ damage: a critical appraisal of the literature using meta-analytic techniques. *Pediatrics* 2003;112:634-40.
 5. Benjamin DK Jr, Stoll BJ, Fanaroff AA, et al. Neonatal candidiasis among extremely low birth weight infants: risk factors, mortality rates, and neurodevelopmental outcomes at 18 to 22 months. *Pediatrics* 2006;117:84-92.
 6. Sánchez-Portocarrero J, Pérez-Cecilia E, Corral O, et al. The central nervous system and infection by *Candida* species. *Diagn Microbiol Infect Dis* 2000;37:169-79.
 7. Moylett EH. Neonatal *Candida* meningitis. *Semin Pediatr Infect Dis* 2003;14:115-22.
 8. Faix RG, Chapman RL. Central nervous system candidiasis in the high-risk neonate. *Semin Perinatol* 2003;27:384-92.
 9. Smith PB, Garges HP, Cotton CM, et al. Meningitis in preterm neonates: importance of cerebrospinal fluid parameters. *Am J Perinatol* 2008;25:421-6.
 10. Bozynski ME, Naglie RA, Russell EJ. Real-time ultrasonographic surveillance in the detection of CNS involvement in systemic *Candida* infection. *Pediatr Radiol* 1986;16:235-7.
 11. Tung KT, MacDonald LM, Smith JC. Neonatal systemic candidiasis diagnosed by ultrasound. *Acta Radiol* 1990;31:293-5.
 12. Wong KK, Gruenewald SM, Larcos G, et al. Neonatal fungal ventriculitis. *J Clin Ultrasound* 2006;34:402-6.
 13. Huang CC, Chen CY, Yang HB, et al. Central nervous system candidiasis in very low-birth-weight premature neonates and infants: US characteristics and histopathologic and MR imaging correlates in five patients. *Radiology* 1998;209:49-56.
 14. Ferrari P, Chiarolanza J, Capriotti T, et al. Favorable course of cerebral candidiasis in a low-birth newborn treated with liposomal amphotericin B. *Pediatr Med Chir* 2001;23:197-9.
 15. Pahud BA, Greenhow TL, Picuch B, et al. Preterm neonates with candidal brain microabscesses: a case series. *J Perinatol* 2009;29:323-6.
 16. Binning MJ, Lee J, Thorell EA, et al. Intraventricular fungus ball: a unique manifestation of refractory intracranial candidiasis in an immunocompetent neonate. *J Neurosurg Pediatr* 2009;4:584-7.
 17. López Sastre JB, Coto Cotallo GD, Fernández Colomer B, et al. Neonatal invasive candidiasis: a prospective multicenter study of 118 cases. *Am J Perinatol* 2003;20:153-63.
 18. Fernandez M, Moylett EH, Noyola DE, et al. Candidal meningitis in neonates: a 10-year review. *Clin Infect Dis* 2000;31:458-63.
 19. Benjamin DK Jr, Poole C, Steinbach WJ, et al. Neonatal candidemia and end-organ damage: a critical appraisal of the literature using meta-analytic techniques. *Pediatrics* 2003;112:634-40.
 20. Lee BE, Cheung PY, Robinson JL, et al. Comparative study of mortality and morbidity in premature infants (birth weight, < 1,250 g) with candidemia or candidal meningitis. *Clin Infect Dis* 1998;27:559-65.
 21. Pendlebury WW, Perl DP, Munoz DG. Multiple microabscesses in the central nervous system: a clinicopathologic study. *J Neuropathol Exp Neurol* 1989;48:290-300.
 22. Lai PH, Lin SM, Pan HB, et al. Disseminated miliary cerebral candidiasis. *AJNR Am J Neuroradiol* 1997;18:1303-6.
 23. Friedman S, Richardson SE, Jacobs SE, et al. Systemic *Candida* infection in extremely low birth weight infants: short term morbidity and long term neurodevelopmental outcome. *Pediatr Infect Dis J* 2000;19:499-504.
 24. Jong AY, Stins MF, Huang SH, et al. Traversal of *Candida albicans* across human blood-brain barrier in vitro. *Infect Immun* 2001;69:4536-44.
 25. Becker LE. Infections of the developing brain. *AJNR Am J Neuroradiol.* 1992;13:537-49.
 26. Chang KH, Han MH, Roh JK, et al. Gd-DTPA enhanced MR imaging in intracranial tuberculosis. *Neuroradiology* 1990;32:19-25.
 27. Mueller-Mang C, Castillo M, Mang TG, et al. Fungal versus bacterial brain abscesses: is diffusion-weighted MR imaging a useful tool in the differential diagnosis? *Neuroradiology* 2007;49:651-7.

Cite this article as: Mao J, Li J, Chen D, Zhang J, Du YN, Wang YJ, Li X, Wang R, Chen LY, Wang XM. MRI-DWI improves the early diagnosis of brain abscess induced by *Candida albicans* in preterm infants. *Transl Pediatr* 2012;1(2):76-84. doi: 10.3978/j.issn.2224-4336.2012.02.04